Quantum atomic dynamics in amorphous silicon; a path-integral Monte Carlo simulation

2000 J. Phys.: Condens. Matter 12 265

(http://iopscience.iop.org/0953-8984/12/3/305)

J. Phys.: Condens. Matter **12** (2000) 265–274. Printed in the UK PII: S0953-8984(00)05948-8

Quantum atomic dynamics in amorphous silicon; a path-integral Monte Carlo simulation

Carlos P Herrero

Instituto de Ciencia de Materiales, Consejo Superior de Investigaciones Científicas (CSIC), Campus de Cantoblanco, 28049 Madrid, Spain

Received 12 June 1999

Abstract. The quantum dynamics of atoms in amorphous silicon has been addressed by using path-integral Monte Carlo simulations. Structural results (radial distribution functions) found from these simulations agree well with experimental data. We study the quantum delocalization of the silicon atoms around their equilibrium positions. This delocalization is larger for coordination defects (fivefold-coordinated Si atoms). Correlations in the atomic displacements are analysed as a function of the interatomic distance and compared with those derived from classical Monte Carlo simulations. At high temperatures, the classical limit is recovered. Our results are also compared with those derived from similar quantum simulations for crystalline silicon. Structural disorder favours a larger vibrational amplitude for the atoms in amorphous silicon.

1. Introduction

The dynamics of atoms in amorphous solids gives rise to localized low-energy excitations, displaying patterns that show a substantial deviation from the situation of atomic nuclei harmonically vibrating around their potential minima [1, 2]. This important deviation from harmonicity in amorphous materials, along with the quantum character of the atomic dynamics, is of great importance in their characterization. In this context, the classical papers by Phillips [3] and Anderson *et al* [4] opened a prolific line of research by modelling the low-energy excitations in amorphous solids by two-level systems. There appeared later several detailed descriptions of the low-energy motion in this kind of material, beyond the standard tunnelling model [5].

Amorphous silicon (a-Si), in addition to its technological importance, is considered as a model system for analysing energy-minimized structures and low-energy excitations in disordered solids [6, 7]. Computer modelling has been extensively used in the last few years to study several structural and dynamical properties of this material [8, 9]. Most simulations were carried out by means of molecular dynamics (MD), using empirical interatomic potentials [10–14]. The most widely employed potential has been that proposed by Stillinger and Weber (SW) [15], which gives a good description of amorphous and crystalline silicon (c-Si). This interatomic potential has been employed in quantum simulations of c-Si, yielding results (quantum delocalization of the Si atoms, heat capacity, thermal expansion) that were in good agreement with those derived from experiment [16, 17]. The vibrational density of states (VDOS) corresponding to the SW potential, as well as its comparison with experimental results, has been studied in detail for c-Si and a-Si [11, 13, 18]. Other empirical potentials for

0953-8984/00/030265+10$30.00

silicon appeared later in the literature [19–22], as well as computational methods for obtaining amorphous structures with low concentrations of coordination defects [23].

Amorphous silicon has been also studied by *ab initio* MD simulations, by using the Car–Parrinello method [24, 25]. This procedure gave good agreement with experiment for the electronic properties and phonon spectrum of a-Si. However, the silicon nuclei are treated in this method as classical particles, and the atomic quantum dynamics can be studied by assuming a harmonic model, with the standard quantization of the solid vibrations. This approach is questionable for studying vibrational properties of amorphous solids, due to the presence of highly anharmonic low-energy vibrations in this kind of material [5]. Even for crystalline solids, vibrational modes are never totally harmonic, and anharmonic terms appear to higher order when expanding in the amplitude of the lattice modes [26]. The contribution of the anharmonic terms in the potential energy becomes more prominent as the phonon coordinate becomes large at finite temperatures.

Finite-temperature properties of solids, beyond the usual harmonic approximation, can be studied by the Feynman path-integral (PI) method, which provides us with a well-suited formulation for the statistical mechanics of quantum systems. By combining numerical methods, such as Monte Carlo (MC) or MD simulations, with the PI formulation, one has a practical way to analyse properties related to the quantum nature of the atomic nuclei. This computational technique is well established as a tool for studying many-body problems in which anharmonic effects can be non-negligible. In our context, static and dynamical properties of c-Si [16, 17] and of point defects in this material were studied earlier by using PI MC simulations [27, 28]. Recently, we have shown that quantum effects in the delocalization of the atomic nuclei are non-negligible also in the presence of structural disorder [29]. This means, in particular, that the peaks in the radial distribution function (RDF) of a-Si can be broadened by zero-point motion of the silicon nuclei. In line with this, the present work is an extension of the results presented earlier in reference [29].

In this paper we present a PI MC simulation of a-Si, with emphasis on the quantum dynamics and delocalization of the atoms around the potential minima. We analyse the correlation between atom displacements, and compare the results of the quantum simulations with those found from classical Monte Carlo simulations, as well as with those obtained for c-Si with the same method.

2. Computational method

For our system of P quantum particles (Si nuclei), the partition function Z at temperature T can be written as a path integral in the following way [30]:

$$Z = \int \exp\left[-\frac{1}{\bar{h}}\int_0^{\beta\bar{h}} \Phi[\boldsymbol{R}(\tau)]\,\mathrm{d}\tau\right]\mathcal{D}\boldsymbol{R}(\tau) \tag{1}$$

where $\beta = 1/(k_B T)$, τ is the so-called imaginary time, and $\boldsymbol{R}$ is a vector in a $3P$-dimensional space, the components of which are the Cartesian coordinates of the nuclei, $\boldsymbol{R} = (\boldsymbol{r}_1, \ldots, \boldsymbol{r}_P)$. The paths $\boldsymbol{R}(\tau)$ fulfil the cyclic condition $\boldsymbol{R}(0) = \boldsymbol{R}(\beta\bar{h})$, and the function $\Phi[\boldsymbol{R}(\tau)]$ is given by

$$\Phi[\boldsymbol{R}(\tau)] = \frac{1}{2}m\sum_{p=1}^{P}\dot{\boldsymbol{r}}_p^2(\tau) + V[\boldsymbol{R}(\tau)] \tag{2}$$

where m is the Si nuclear mass, and $\dot{\boldsymbol{r}}_p$ the derivative of $\boldsymbol{r}_p$ with respect to the imaginary time τ. Our calculations are carried out within the Born–Oppenheimer approximation, and we employ a potential energy surface $V(\boldsymbol{R})$ for the nuclei coordinates, as described below.

The path integral in equation (1) can be evaluated by a discretization of the paths $\boldsymbol{R}(\tau)$ into N points $(\boldsymbol{R}_1, \boldsymbol{R}_2, \ldots, \boldsymbol{R}_N)$. For sufficiently large N (the so-called Trotter number), Z can be approximated by a free-particle propagator, leading to the expression [31]

$$Z_N = \left(\frac{Nm}{2\pi\beta\overline{h}^2}\right)^{3PN/2} \int \mathrm{d}\boldsymbol{R}_1 \cdots \mathrm{d}\boldsymbol{R}_N \ \exp(-\beta V_{\mathrm{eff}}) \tag{3}$$

where the integral is extended to the whole $3P$-dimensional configuration space. Z_N is formally equivalent to the partition function for a classical system of P cyclic 'chains', interacting via an effective potential $V_{\mathrm{eff}}(\boldsymbol{R}_1, \ldots, \boldsymbol{R}_N)$, and each 'chain' being divided into N 'time slices'. This causes the appearance in the simulations of N 'replicas' for each quantum particle. Such replicas are treated as classical particles, and the corresponding partition function Z_N converges to Z in the limit $N \to \infty$ [31]. More details on this method can be found elsewhere [31, 32].

The interatomic interaction has been modelled by the SW potential [15]. We have employed for amorphous silicon a cubic cell including 216 Si atoms, with a length of 16.6 Å and periodic boundary conditions. This simulation cell was generated by a simulated annealing process, using classical MC simulations, as described elsewhere [10, 13, 29]. For the sake of comparison, we have performed also MC simulations of c-Si, under the same conditions as those for a-Si. For the crystalline material, we have employed a $2 \times 2 \times 2$ supercell of the regular face-centred-cubic cell, as described elsewhere [16].

Path-integral Monte Carlo simulations of a-Si and c-Si were carried out in the temperature range from 10 to 800 K. The Trotter number N was made temperature dependent: $N = 3\beta\overline{h}\omega_0$ with $\omega_0 = 450\ \mathrm{cm}^{-1}$, close to the Debye frequency of the material. For example, at 50 K we have $N = 40$ replicas for the Si nuclei. For a few temperatures, we have checked that the use of larger values for N does not produce any appreciable change in the results presented here for a-Si, in line with earlier findings for c-Si [16]. Thus, the numerical error introduced in the energy by the discretization of the path integrals is lower than ± 0.3 meV per Si atom, over the whole temperature range studied here.

The partition function Z_N in equation (3) has been sampled by the Metropolis method [33, 34]. A simulation run proceeds via successive MC steps, each one consisting of sequential moves of: (i) the replicas associated with each nucleus; and (ii) the centre of gravity of the cyclic paths (rigid moves of the paths). At each temperature studied, the maximum distance allowed for random moves was adjusted to yield an acceptance ratio of about 50% for each kind of sampling. With this criterion, at 50 K the maximum change in the Cartesian coordinates in a MC step amounts to 0.059 Å for moves of individual replicas, and to 0.049 Å for centre-of-gravity moves. At 500 K, the corresponding values are 0.058 and 0.156 Å, respectively. For each temperature, we generated 5000 paths per atom for system equilibration, and 20 000 paths per atom for the calculation of ensemble-average properties. For comparison, we have carried out also classical MC simulations of a-Si and c-Si in the same temperature range as the PI MC simulations. This classical limit is in fact obtained by setting the Trotter number $N = 1$ in our calculations.

In the path-integral formalism, the finite mean radius of the cyclic paths is related to a spatial delocalization of the particle, which results from quantum fluctuations. To give a quantitative measure of the spread of the density distribution for a given nucleus p due to quantum fluctuations, we employ the quantum delocalization Q_p^2, defined as the mean square radius of the paths $\boldsymbol{r}_{pj}$:

$$Q_p^2 = \left\langle \frac{1}{N} \sum_{j=1}^{N} (\boldsymbol{r}_{pj} - \overline{\boldsymbol{r}}_p)^2 \right\rangle \tag{4}$$

where the index j indicates the different replicas (time slices) of nucleus p, and the centre of gravity of a path (sometimes called the 'centroid') is given by

$$\overline{\boldsymbol{r}}_p = \frac{1}{N}\sum_{j=1}^{N} \boldsymbol{r}_{pj}. \tag{5}$$

The angular brackets in equation (4) and in the expressions given in the following indicate ensemble averages with the partition function given in equation (3). In the classical limit (high temperatures), the cyclic paths collapse into single points and therefore $Q_p^2 \to 0$.

The quantity Q coincides with the so-called 'radius of gyration' [31, 35], defined for the quantum paths in analogy with classical simulations of solids and fluids (note that we write Q when speaking about quantum particles in general, and Q_p when we refer to a given atomic nucleus p, as in equation (4)). For an isotropic three-dimensional harmonic oscillator with frequency ω, the mean square radius Q_{ho}^2 of the quantum paths is given by [35]

$$Q_{ho}^2 = \frac{3\overline{h}}{2m\omega}\coth\left(\frac{\overline{h}\omega}{2k_BT}\right) - \frac{3k_BT}{m\omega^2} \tag{6}$$

i.e., it coincides with the difference between the total spatial delocalization $(\Delta \boldsymbol{r})^2$ of the quantum oscillator (the first term on the r.h.s. of equation (6)) and the thermal delocalization of a classical oscillator at temperature T (the second term in equation (6)).

In general, one can define a 'thermal' delocalization for a quantum particle at a given temperature T as the mean square displacement of the centre of gravity of its corresponding paths; i.e.,

$$C^2 = \langle \overline{\boldsymbol{r}}^2 \rangle - \langle \overline{\boldsymbol{r}} \rangle^2. \tag{7}$$

For a particle moving around a potential minimum, as is the case here for Si nuclei, this quantity C^2 goes to zero for $T \to 0$ [36], and converges to the classical mean square displacement of the particle at high temperatures. The total spatial delocalization of the quantum particle is given by

$$D^2 \equiv (\Delta \boldsymbol{r})^2 = Q^2 + C^2. \tag{8}$$

Thus, the quantum delocalization of particle (atomic nucleus) p, Q_p^2, calculated as the mean square radius of the paths, coincides in the limit $T \to 0$ with the delocalization $(\Delta \boldsymbol{r}_p)^2$ due to zero-point motion. Note that for the particular case of a harmonic oscillator, C^2 coincides with the classical mean square displacement $3k_BT/m\omega^2$ at any temperature T, but this is not true in general.

3. Results

The structure of amorphous materials is conveniently characterized by the pair correlation or radial distribution function $g(r)$ [1, 2]. In figure 1 we show the RDF for a-Si, as derived from our classical (continuous lines) and quantum (dashed lines) Monte Carlo simulations, in the region of interatomic distances between 2 and 2.8 Å. At T = 50 K (part (a) of the figure), there appears a clear difference between the two curves. In particular, the height of the first peak in the RDF (that corresponding to nearest neighbours) is larger in the classical result than that found from the quantum simulations. For increasing temperature, the width of the peak increases, whereas its height becomes smaller [29]. This change is more pronounced in the classical results, and thus the difference between the RDF obtained in the classical and quantum simulations is reduced as temperature goes up. However, this difference is still observable at T = 400 K, as shown in figure 1(b). The two kinds of Monte Carlo simulation, classical and

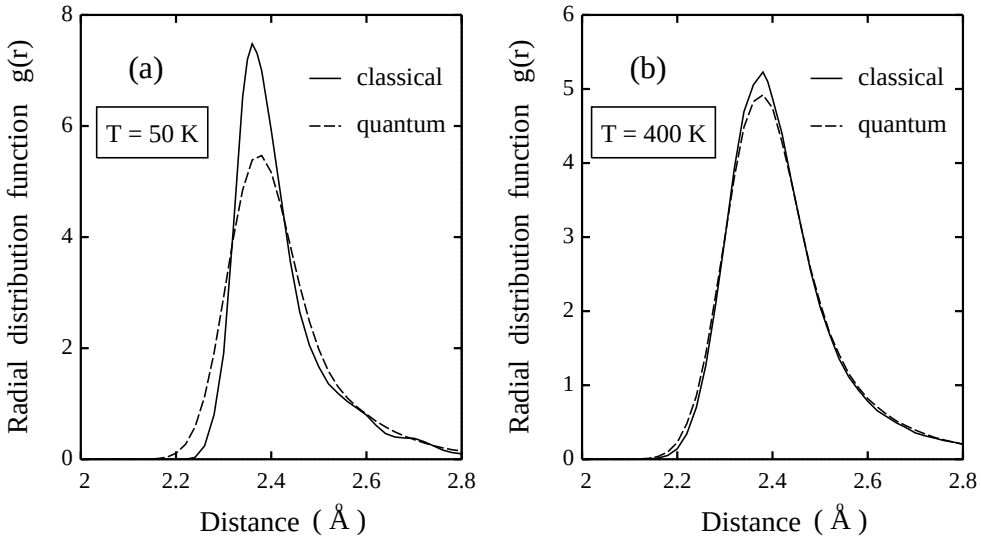

Figure 1. The radial distribution function for amorphous silicon in the region of the nearest-neighbour distance, as derived from quantum (dashed lines) and classical (continuous lines) Monte Carlo simulations, at two different temperatures: (a) T = 50 K; (b) T = 400 K.

quantum, give the same result at temperatures of the order of the Debye temperature of the material ($\Theta_D \sim 650$ K). A comparison of the RDFs found from PI MC simulations of a-Si and c-Si was presented elsewhere [29].

In figure 2 we present a comparison of the RDF derived from our PI MC simulations at room temperature, and that found from neutron diffraction results for pure evaporated amorphous silicon by Kugler *et al* [37]. Note that we present results for $g(r)$, which is related to the radial distribution function $t(r)$ shown in reference [37] by $t(r) = 4\pi d r g(r)$, where d is the density of the material. From our quantum simulations we find a good agreement with the experimental results, taking into account the artifacts appearing in the RDF derived from the experiment, and presumably connected with the Fourier transformation of the measured structure factor $S(Q)$. These artifacts are especially important at small distances (see the feature at $r < 2$ Å in figure 2), due to the cut-off in momentum space.

We now turn to study the spatial delocalization (mean square displacements) of the Si atoms, caused by the vibrational modes in the material. At this point it is convenient to distinguish between fourfold-coordinated Si atoms and coordination defects in the amorphous material, as the latter are expected to show a different vibrational behaviour. Our generated cells for a-Si contain between 10 and 20% fivefold-coordinated atoms (assuming a nearest-neighbour cut-off of 2.9 Å), and they do not include threefold-coordinated ones. The quantum delocalization Q^2 is displayed in figure 3 for low temperatures. Black squares and circles correspond to fourfold- and fivefold-coordinated atoms in a-Si. For comparison, the delocalization Q^2 in c-Si is also given (open squares). The largest difference between the values found for these three cases appears close to $T = 0$. In the low-temperature limit, the radius of gyration for fivefold-coordinated atoms is larger than that corresponding to fourfold-coordinated ones, as a consequence of the larger vibrational density of states at low energies in the coordination defects [38]. In the case of fourfold-coordinated Si atoms, the low-temperature radius of gyration is clearly larger in a-Si than in the crystalline material. This could be expected from the shift towards lower energies that is exhibited by the VDOS of the amorphous material,

as compared to its crystalline counterpart [11, 13, 18]. At temperatures larger than 200 K, the quantum delocalization approaches the high-temperature limit

$$Q^2 = \frac{\hbar^2 \beta}{4m} \tag{9}$$

i.e., it goes as c/T, where c is a constant that depends on the particle mass m, but not on the details of the potential surface.

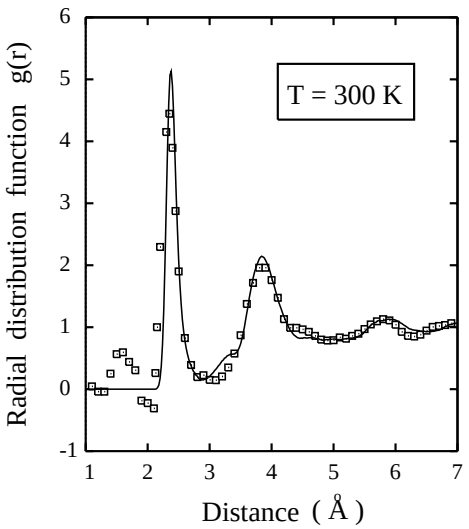

Figure 2. The radial distribution function for amorphous silicon. Symbols are results from neutron diffraction measurements [37], and the continuous line was obtained from PI MC simulations at 300 K.

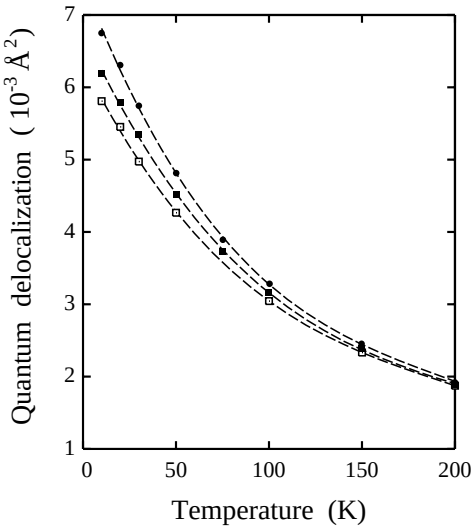

Figure 3. Mean square radius of gyration of the quantum paths for fourfold- (black squares) and fivefold- (black circles) coordinated atoms in a-Si, and in c-Si (open squares). Lines are guides to the eye.

As explained above, the decrease in quantum delocalization Q^2, as temperature goes up, is accompanied by an increase in the 'thermal' delocalization of the silicon nuclei (but the sum of the two quantities, D^2, increases with T). The delocalization C^2 is shown in figure 4 as a function of temperature. Black symbols correspond to a-Si (squares and circles for fourfold- and fivefold-coordinated atoms, respectively), whereas open squares are data points obtained for c-Si in the PI MC simulations. As indicated above, this quantity C^2 should follow a linear temperature dependence in a harmonic approach, and deviations from linearity are due to anharmonicities in the potential energy surface around its minima. The dashed lines in figure 4 are linear fits to the low-temperature data for the three different cases shown there. For c-Si (open symbols) the thermal delocalization follows closely a linear behaviour, apart from a slight deviation at temperatures larger than 600 K. Such a departure from linearity is more pronounced for a-Si, and it is most prominent for coordination defects (fivefold-coordinated atoms) at high temperatures, where the thermal delocalization is clearly larger than that expected from the extrapolation of the low-temperature results in a harmonic approach.

The quantum motion of atoms in solids is usually studied within the harmonic approximation by quantization of the vibrational normal modes into phonons. These quantum vibrations describe the relative motion of the atoms at different frequencies and wave vectors. From the path-integral Monte Carlo simulations, one can study the relative displacements of the atoms in real space. In particular, the influence of quantum effects on the atomic motion

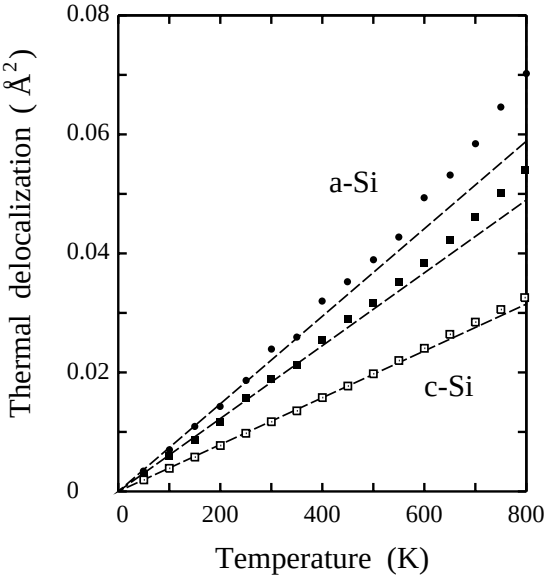

Figure 4. Thermal delocalization C^2 of the Si nuclei versus the temperature. Black squares: fourfold-coordinated atoms in a-Si; black circles: fivefold-coordinated atoms in a-Si; open squares: c-Si. The dashed lines are linear fits to the low-temperature data points.

can be quantified by calculating the correlations between atom displacements at different temperatures. To this end, we define the correlation ρ for displacements of atom pairs by the quantity:

$$\rho_{pq} = \frac{\langle \boldsymbol{u}_p \cdot \boldsymbol{u}_q \rangle}{\left[\langle \boldsymbol{u}_p^2 \rangle \langle \boldsymbol{u}_q^2 \rangle\right]^{1/2}} \tag{10}$$

where $\boldsymbol{u}_p$ ($\boldsymbol{u}_q$) is the displacement of atom p (q) from its equilibrium position. It is clear that ρ_{pq} is a number in the interval [–1, 1]. For atoms vibrating strictly in phase, one has $\rho_{pq} = 1$, and one expects $\rho_{pq} = -1$ when they vibrate in anti-phase. For independent motion of atoms p and q, one would have $\rho_{pq} = 0$. From our path-integral formalism, ρ_{pq} can be calculated as

$$\rho_{pq} = \frac{1}{D_p D_q}\left\langle \frac{1}{N}\sum_{j=1}^{N} (\boldsymbol{r}_{pj} - \langle \overline{\boldsymbol{r}}_p \rangle) \cdot (\boldsymbol{r}_{qj} - \langle \overline{\boldsymbol{r}}_q \rangle) \right\rangle. \tag{11}$$

This correlation is expected to be important for small interatomic distances and will decrease as the interatomic distance increases. This is in fact found from the PI MC simulations, as was shown in reference [29]. For a-Si at room temperature, ρ has the value 0.34 for nearest-neighbour atoms, and is close to zero for $r > 6$ Å. By studying the dependence of the correlation ρ on interatomic distance r, one finds that it does not depend appreciably on the degree of structural disorder present in the material, since the results obtained for amorphous and crystalline silicon are similar for a given distance r [29].

The temperature dependence of the correlation ρ for nearest neighbours is shown in figure 5 for amorphous (part (a)) and crystalline silicon (part (b)). For each material, we present results from classical and quantum Monte Carlo simulations. In the classical simulations, one finds, for both a-Si and c-Si, that ρ is roughly independent of temperature, and coincides with the high-temperature limit of the quantum simulations. Note that these classical results for a-Si (black squares) are slightly (but clearly) lower than those corresponding to c-Si (open squares). This is a consequence of the fact that the average nearest-neighbour distance in a-Si is larger than in c-Si, due to the asymmetry in the first peak in the RDF of a-Si (see figure 1). Since ρ decreases for increasing r, one expects for a-Si an average value lower than for c-Si, when

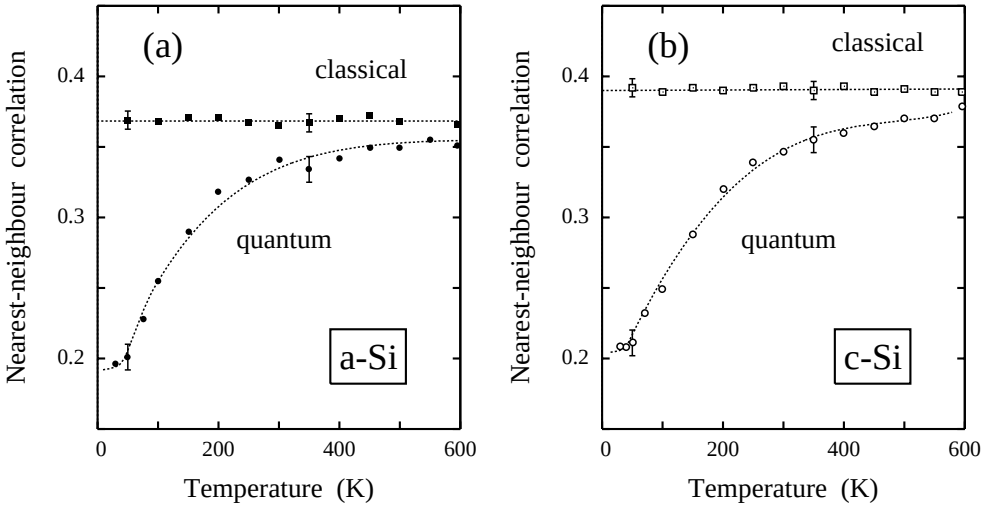

Figure 5. The temperature dependence of the correlation ρ between atom displacements for nearest neighbours: (a) amorphous silicon; (b) crystalline silicon. Squares and circles correspond to results derived from classical and quantum Monte Carlo simulations, respectively. Lines are guides to the eye.

integrating ρ for nearest neighbours (we have used a nearest-neighbour cut-off distance of 2.9 Å).

In a classical harmonic approximation, because of the equipartition principle one has $\langle \boldsymbol{u}_p \cdot \boldsymbol{u}_q \rangle = A_{pq} T$, where A_{pq} is a constant independent of temperature. Thus, ρ_{pq} is temperature-independent in such a classical approach. This is what we find for the correlation ρ_{pq} from our classical MC simulations for a-Si and c-Si, indicating that the anharmonicities in the vibrational modes do not affect this correlation in practice. Although both $\langle \boldsymbol{u}_p^2 \rangle$ and $\langle \boldsymbol{u}_q^2 \rangle$ in the denominator of equation (10) show clear deviations from the linear behaviour expected for a harmonic approach (especially at high T; see, e.g., figure 4), these deviations are compensated for by those appearing in $\langle \boldsymbol{u}_p \cdot \boldsymbol{u}_q \rangle$ in the numerator of that expression.

In a quantum model of the lattice vibrations, however, ρ_{pq} should depend on temperature, as different vibrational modes have different relative contributions, depending on the frequency ω and the temperature T. In particular, for a harmonic approach, the contribution to $\langle \boldsymbol{u}_p \cdot \boldsymbol{u}_q \rangle$ of a mode with frequency ω will be proportional to $[\bar{n}(\omega, T) + 1/2]/\omega$, where $\bar{n}(\omega, T)$ is the Bose–Einstein thermal population factor. This means that at zero temperature this contribution scales as $1/\omega$, whereas at high T it goes as $1/\omega^2$. Then, the relative weight of modes with small ω increases for increasing temperature. The low-frequency part ($\omega \lesssim 200$ cm^{-1}) of the vibrational spectrum is dominated by long-wavelength (acoustic) modes. These modes have a positive (close to 1) contribution to the correlation ρ_{pq} between neighbouring atoms, and thus their enhancing contribution for increasing temperature causes ρ_{pq} to become larger. This is basically what one observes in figure 5 for a-Si (closed circles) and c-Si (open circles).

4. Concluding remarks

We have shown that quantum atomistic simulations of amorphous materials, and silicon in particular, are complementary to the classical simulations (MC and MD) carried out in the last decade. Path-integral MC simulations are especially interesting, since they provide us with

detailed information on microscopic properties of these materials, that are directly influenced by the presence of structural disorder and anharmonicity in the solid vibrations. As expected, quantum corrections to the atom delocalization, and thereby to structural characteristics such as the radial distribution function, become non-negligible at temperatures lower than the Debye temperature of the material ($\Theta_D \sim 650$ K).

We have studied the mean square displacement of the atomic vibrational motion. In particular, the spatial extent of the quantum paths that describe the Si nuclei at a temperature T gives the quantum delocalization Q^2. This quantity is a measure of the relevance of quantum effects in describing the atom dynamics. It converges to the mean square displacement $(\Delta \boldsymbol{r})^2$ at $T = 0$, and is larger for fivefold-coordinated atoms, as expected for quantum particles with a larger density of low-energy vibrations. Even small extra contributions of low-frequency modes to the VDOS can have an appreciable effect on the atom delocalization. The 'thermal' delocalization C^2 is also larger for the coordination defects. For C^2, the contribution of low-frequency modes is particularly important at high T, whereas for D^2 it is most relevant at low temperatures. Thus, the increase in atomic delocalization in a-Si, as compared with c-Si, is caused by a softening of the vibrational modes and a larger anharmonicity in the amorphous solid.

These real-space quantum simulations allow us to study correlations in the actual motion of neighbouring atoms. For a given interatomic distance r, the correlation $\rho(r)$ becomes smaller for decreasing temperature. This is due to the quantum delocalization, that dominates at low temperatures (versus the thermal delocalization), and causes a decrease in the correlation of atom displacements, as compared with the classical result.

A limitation of the computational method employed here is the use of effective interatomic potentials, fitted to reproduce known properties of the material. In connection with this, we note that, in recent years, *ab initio* PI molecular dynamics simulations have been carried out for molecules [39], and they begin now to be feasible for studying certain properties of solids [40].

Quantum simulations such as those presented here can give valuable information on several challenging problems related to amorphous semiconductors. In particular, the microscopic structure and atomic dynamics in hydrogenated amorphous silicon are interesting questions, whose study has to involve the presence of structural disorder (and thereby enhanced anharmonicities) and light atoms, which renders the treatment of quantum effects (hydrogen delocalization, tunnelling) highly non-trivial.

Acknowledgments

This work was supported by CICYT (Spain) under Contract No PB96-0874. Helpful discussions with R Ramírez and M A Ramos are acknowledged.

References

[1] Cusack N E 1987 *The Physics of Structurally Disordered Matter* (Bristol: Hilger)
[2] Elliott S R 1990 *Physics of Amorphous Materials* (New York: Longman)
[3] Phillips W A 1972 *J. Low Temp. Phys.* **7** 351
[4] Anderson P W, Halperin B I and Varma C M 1972 *Phil. Mag.* **25** 1
[5] Ramos M A and Buchenau U 1998 *Tunnelling Systems in Amorphous and Crystalline Solids* ed P Esquinazi (Berlin: Springer)
[6] Barkema G T and Mousseau N 1996 *Phys. Rev. Lett.* **77** 4358
[7] Liu X, White B E, Pohl R O, Iwanizcko E, Jones K M, Mahan A H, Nelson B N, Crandall R S and Veprek S 1997 *Phys. Rev. Lett.* **78** 4418
[8] Wooten F, Winer K and Weaire D 1985 *Phys. Rev. Lett.* **54** 1392

[9] Wooten F and Weaire D 1987 *Solid State Physics* vol 40 (New York: Academic) p 1
[10] Kluge M D, Ray J R and Rahman A 1987 *Phys. Rev.* B **36** 4234
[11] Kluge M D and Ray J R 1988 *Phys. Rev.* B **37** 4132
[12] Biswas R, Grest G S and Soukoulis C M 1987 *Phys. Rev.* B **36** 7437
[13] Luedtke W D and Landman U 1989 *Phys. Rev.* B **40** 1164
[14] Cook S J and Clancy P 1993 *Phys. Rev.* B **47** 7686
[15] Stillinger F H and Weber T A 1985 *Phys. Rev.* B **31** 5262
[16] Ramírez R and Herrero C P 1993 *Phys. Rev.* B **48** 14 659
[17] Noya J C, Herrero C P and Ramírez R 1996 *Phys. Rev.* B **53** 9869
[18] Luedtke W D and Landman U 1988 *Phys. Rev.* B **37** 4656
[19] Tersoff J 1988 *Phys. Rev.* B **37** 6991
Tersoff J 1988 *Phys. Rev.* B **38** 9902
[20] Biswas R and Hamman D R 1987 *Phys. Rev.* B **36** 6434
[21] Bazant M Z, Kaxiras E and Justo J F 1997 *Phys. Rev.* B **56** 8542
[22] Justo J F, Bazant M Z, Kaxiras E, Bulatov V V and Yip S 1998 *Phys. Rev.* B **58** 2539
[23] Mousseau N and Lewis L J 1997 *Phys. Rev. Lett.* **78** 1484
[24] Car R and Parrinello M 1988 *Phys. Rev. Lett.* **60** 204
[25] Drabold D A, Fedders P A, Klemm S and Sankey O F 1991 *Phys. Rev. Lett.* **67** 2179
[26] Srivastava G P 1990 *The Physics of Phonons* (Bristol: Hilger)
[27] Ramírez R and Herrero C P 1994 *Phys. Rev. Lett.* **73** 126
[28] Herrero C P and Ramírez R 1995 *Phys. Rev.* B **51** 16 761
[29] Herrero C P 1998 *Europhys. Lett.* **44** 734
[30] Feynman R P 1972 *Statistical Mechanics* (New York: Addison-Wesley)
[31] Gillan M J 1988 *Phil. Mag.* A **58** 257
[32] Ceperley D M 1995 *Rev. Mod. Phys.* **67** 279
[33] Metropolis N, Rosenbluth A W, Rosenbluth M N, Teller A H and Teller E 1953 *J. Chem. Phys.* **21** 20
[34] Binder K and Heermann D W 1988 *Monte Carlo Simulation in Statistical Physics* (Berlin: Springer)
[35] Gillan M J 1990 *Computer Modelling of Fluids, Polymers and Solids* ed C R A Catlow, S C Parker and M P Allen (Dordrecht: Kluwer)
[36] Ramírez R, López-Ciudad T and Noya J C 1998 *Phys. Rev. Lett.* **81** 3303
[37] Kugler S, Molnár G, Petö G, Zsoldos E, Rosta L, Menelle A and Bellissent R 1989 *Phys. Rev.* B **40** 8030
[38] Biswas R, Bouchard A M, Kamitakahara W A, Grest G S and Soukoulis C M 1988 *Phys. Rev. Lett.* **22** 2280
[39] Marx D and Parrinello M 1995 *Nature* **375** 216
[40] Benoit M, Marx D and Parrinello M 1998 *Nature* **392** 258